



VITICULTURE ORIGINAL RESEARCH ARTICLES

Moving beyond visible flower counting: RGB image-based flower number and yield prediction in grapevine

Stefano Puccio¹, Daniele Micciché^{1,*}, Rosario Di Lorenzo¹, Lucia Turano¹, and Antonino Pisciotta¹

¹ Department of Agricultural, Food and Forest Sciences (SAAF), University of Palermo, Viale delle Scienze 11 build. H - 90128 Palermo, Italy

Article number: 9210



*correspondence:
daniele.micciche@unipa.it

Associate editor:
Bruno Tisseyre



Received:
26 February 2025

Accepted:
4 August 2025

Published:
4 September 2025



This article is published under the **Creative Commons licence** (CC BY 4.0).

Use of all or part of the content of this article must mention the authors, the year of publication, the title, the name of the journal, the volume, the pages and the DOI in compliance with the information given above.

ABSTRACT

Accurate yield estimation is crucial for optimising vineyard management and logistical organisation. Traditional methods relying on manual and destructive flower or berry counts are labour-intensive and unsuitable for large-scale applications. To address these limitations, this study evaluated the potential of RGB image analysis for non-destructive estimation of flower number in grapevine inflorescences and its relationship with yield components. The objectives were: (i) to correlate the number of actual flowers with the number of pixels in inflorescence images, considering the projected area and not visible flower count; (ii) to assess the model's ability for predicting yield components (number of berries and bunch weight) on the plant scale. The study was conducted during the 2023 vintage in a cv. Catarratto/1103P vineyard located in Sicily, on 36 vines. The vines were trained on a vertical shoot positioning trellis system with a bilateral spur pruned cordon. All the inflorescence images were acquired using a smartphone and white cardboard under field conditions. Images were analysed using FIJI/ImageJ© software, inflorescences were segmented *via* Otsu's method, and pixel counts were used to estimate flower number through linear regression. Flower counts were validated through manual counts of detached calyptra. Vines were harvested to measure bunch weight, and the number of berries was counted to calculate the fruit set rate. External model validation was performed on datasets from Catarratto, Chardonnay, and Vermentino cvs. Results showed a strong correlation between inflorescence pixel count and flower number, both on single inflorescences ($R^2 = 0.78$; MAPE 29 %; $n = 300$) and in terms of total flowers per vine ($R^2 = 0.95$; MAPE 12 %), with estimation accuracy slightly varying according to inflorescence length. External validation yielded an MAPE of 20 % in Catarratto, 40 % in Chardonnay, and 34 % in Vermentino. The model also reliably predicted the number of berries ($R^2 = 0.94$; MAPE 13 %) and bunch weight ($R^2 = 0.79$; MAPE 20 %) per vine. While environmental factors such as fruit set can affect yield, this study highlights the potential for early yield prediction with image analysis. The methodology holds promise for scalable applications and integration into vineyard management technologies in wine and table grapes.

KEYWORDS: computer vision, *Vitis vinifera* L., linear regression, berry number, bunch mass weight

INTRODUCTION

Accurately estimating vineyard yield provides numerous benefits, allowing for the optimisation of both grape quality and quantity. This facilitates oenological management and improves vineyard operations. When done early, yield estimation enables adjustments to grape production in line with oenological objectives while ensuring efficient cellar logistics (Kliewer & Dokoozlian, 2005; Dunn & Martin, 2004; Kliewer & Casteel, 2003). In addition to these benefits, early yield estimation provides valuable information for managing vineyard operations such as summer pruning, bunch thinning, fertilisation, and irrigation (Howell, 2001). Traditional yield estimation methods rely on destructive and manual techniques, which limit their application to a small number of samples. These methods require manually counting flowers, bunches, and berries, which is an approach that is both labour-intensive and impractical on a large scale (Lopes *et al.*, 2021; Carrillo *et al.*, 2016; De La Fuente *et al.*, 2015; Nuske *et al.*, 2014). To overcome these limitations, precision viticulture is advancing toward the development of non-destructive methodologies using cost-effective instrumentation, enabling a broader and more accurate yield assessment. Several studies have explored yield prediction through image analysis, including methods based on counting bunch number and weight (Poblete-Echeverria *et al.*, 2025; Diago *et al.*, 2015; Liu & Whitty, 2015; Font *et al.*, 2014), number and biomass of shoots (Moreno *et al.*, 2020; Demestihis *et al.*, 2018; Liu, 2017), and number of berries within bunches (Aquino *et al.*, 2018; Millan *et al.*, 2018). Other approaches combine the counting of shoots, inflorescences, and bunches at different phenological stages (Victorino *et al.*, 2020), further improving prediction accuracy. Several other techniques have also been investigated, including Synthetic Aperture Radar (SAR), low-frequency ultrasound (Parr *et al.*, 2020), radio-frequency (RF) signals (Altherwy & McCann, 2020), frequency-modulated continuous-wave (FMCW) radar (Henry *et al.*, 2019), and the integration of RGB and multispectral imagery combined with occlusion ratio analysis (Fernandez *et al.*, 2013). However, obtaining early data on the number of flowers per inflorescence would provide an even greater advantage. This is because several key factors that define the bunch, such as the number of berries, bunch weight, and fruit set rate, are directly linked to flower count, allowing for more comprehensive monitoring. Additionally, acquiring this information at an earlier stage not only facilitates logistical planning but also enables the timely and more precise implementation of key canopy and crop management practices—such as shoot thinning, bunch thinning, and summer pruning. When properly timed and calibrated, these interventions can significantly affect vine balance, fruit set, and ultimately influence both yield potential and fruit quality (Keller, 2010; Howell, 2001; May, 2004). While approximately 65 % of the annual variation in grape yield is determined by the number of bunches, the remaining 35 % is linked to the number of berries per bunch, which is directly influenced by the number

of flowers (Clingeffer, 2010; Clingeffer & Krstic, 2003). To address the challenge of manually counting individual flowers, several alternative methods have been proposed over the years. These include manually counting flowers in the first wing of the inflorescence (Bennett *et al.*, 2005), counting the number of wings per inflorescence (Dunn & Martin, 2007), or even counting visible flowers from printed images of inflorescences (Poni *et al.*, 2006). However, these approaches remain destructive and/or labour-intensive, limiting their application to a small number of inflorescences. Some researchers have demonstrated that estimating the number of visible flowers through computer-based image analysis is possible. Diago *et al.* (2014) proposed a methodology later applied by Aquino *et al.* (2015a) in the development of a smartphone application. Their approach, based on images of inflorescences, uses a technique called H-maxima transform, which identifies bright spots in images to count flowers. By leveraging the higher light reflectance of visible flower buds compared to other elements in the image, this method detects points of maximum brightness and automatically counts them, providing an accurate correlation with the actual number of flowers. Building on the same principle, Aquino *et al.* (2015b) developed an algorithm based on image morphological analysis and pyramidal decomposition, capable of operating without artificial backgrounds in vineyard-acquired images. Other studies have introduced models that account for multiple variables and different cultivars. For instance, Millan *et al.* (2017) proposed simple models that predict bunch weight based on the number of visible flowers and average berry weight. The same algorithm was later applied by Palacios *et al.* (2020) to analyse images captured on the go, with the additional goal of predicting yield per plant. Liu *et al.* (2018) took a different approach, applying a method based on inflorescence image segmentation at various phenological stages. Using morphological filters, they aimed to isolate visible flower buds by separating them from other image elements through the Watershed algorithm. Similarly, Benmehaia *et al.* (2016) studied table grape inflorescences. Tello *et al.* (2020) investigated the relationship between flower number and inflorescence density, highlighting how flower estimation models could be improved by incorporating this parameter into multiple regression models. However, all the cited studies on image analysis have exclusively focused on the correlation between the number of visible flowers and the actual number of flowers. As noted by Bessis (1960), there is a linear relationship between length, inflorescence density, and flower quantity. This relationship was further explored by Liu *et al.* (2018), whose results confirm that inflorescence density is a critical factor for achieving positive outcomes in image analysis. This principle is also supported by other studies focused on estimating the number of berries per bunch (Victorino *et al.*, 2022; Lopes & Cadima, 2021; Tello *et al.*, 2018; Cubero *et al.*, 2015). Since the number of flowers is linked to inflorescence length, the size and shape of the inflorescence influence the area captured in images taken with an RGB camera. Based on these considerations, the study had two main objectives: (i) to investigate the

correlation between the actual number of flowers and the number of pixels in inflorescence images, taking into account the projected area rather than the visible flower count, and to evaluate the influence of inflorescence length on the accuracy of the estimation method; (ii) to evaluate the applicability of the model for estimating other yield-related parameters, such as the number of berries per plant and the total bunch mass per plant.

MATERIALS AND METHODS

1. Experimental design and image acquisition

The trial was conducted in 2023 in a vineyard of the cultivar Catarratto/1103P (*Vitis vinifera* L.) located in Camporeale (37° 55' 12.82" N 13° 04' 28.33" E; 320 m a.s.l.; Palermo, Italy), in the Alcamo D.O.C. area. The vines were trained in on a vertical shoot positioning trellis system with two pairs of movable wires with a bilateral spurred cordon, irrigated through a drip irrigation system (dripper flow rate of 2 L/h; distance between drippers 80 cm) on a loamy-clay soil. Planting distances were 0.9 m on the row and 2.2 m between rows, with north-east/south-west orientated rows. Phytosanitary, canopy, and fertilisation management were applied according to standard viticultural practices of an organic vineyard. During winter 2022, 36 grapevines were selected and marked based on their variability in vigour, as identified through NDVI values extracted from multispectral images acquired during flowering and ripening in the previous season. The selection was subsequently validated by measuring the weight of pruned wood. At the pre-flowering stage (BBCH 55), all inflorescences ($n = 300$) were measured

and labelled on each plant. Each inflorescence was assigned to a unique code for later traceability once the bunch was removed. For each inflorescence, the length of the rachis from the insertion point of the first wing to the last visible floral button at the distal end was measured. In cases where the first wing was particularly pronounced, the length of the inflorescence was taken as the sum of the wing length and the rachis. To classify the inflorescences into six categories, a range of lengths was established based on observed variation in inflorescence size, with each category representing a specific length interval: A, $L < 6$ cm; B, $6 \leq L < 8$ cm; C, $8 \leq L < 10$ cm; D, $10 \leq L < 12$ cm; E, $12 \leq L < 14$ cm; F, $L \geq 14$ cm. Image acquisition took place at the BBCH 55 stage according to the Lorenz scale (Lorenz *et al.*, 1995), in accordance with Liu *et al.* (2018), who identified this phenological stage as the most stable and suitable for capturing images of wine grapevine inflorescences for digital analysis. At this stage, the inflorescence shape is relatively consistent, whereas as the season progresses and inflorescence length increases, the shape can change, potentially altering the relationship between length and the number of flowers (May, 2000; Bessis, 1960). Images were acquired in the field between 8:00 am and 2:00 pm under variable and uncontrolled lighting conditions, using a white cardboard sheet behind the inflorescences to standardise the background. The images were captured with a common smartphone camera (Sony Xperia 1 VI, SONY, Japan) using default automatic settings ($f/1.8$ aperture and 26 mm focal length), with no flash. The inflorescences were photographed along an orthogonal axis at 20 cm, measured using a graduated ruler as a reference (Figure 1).

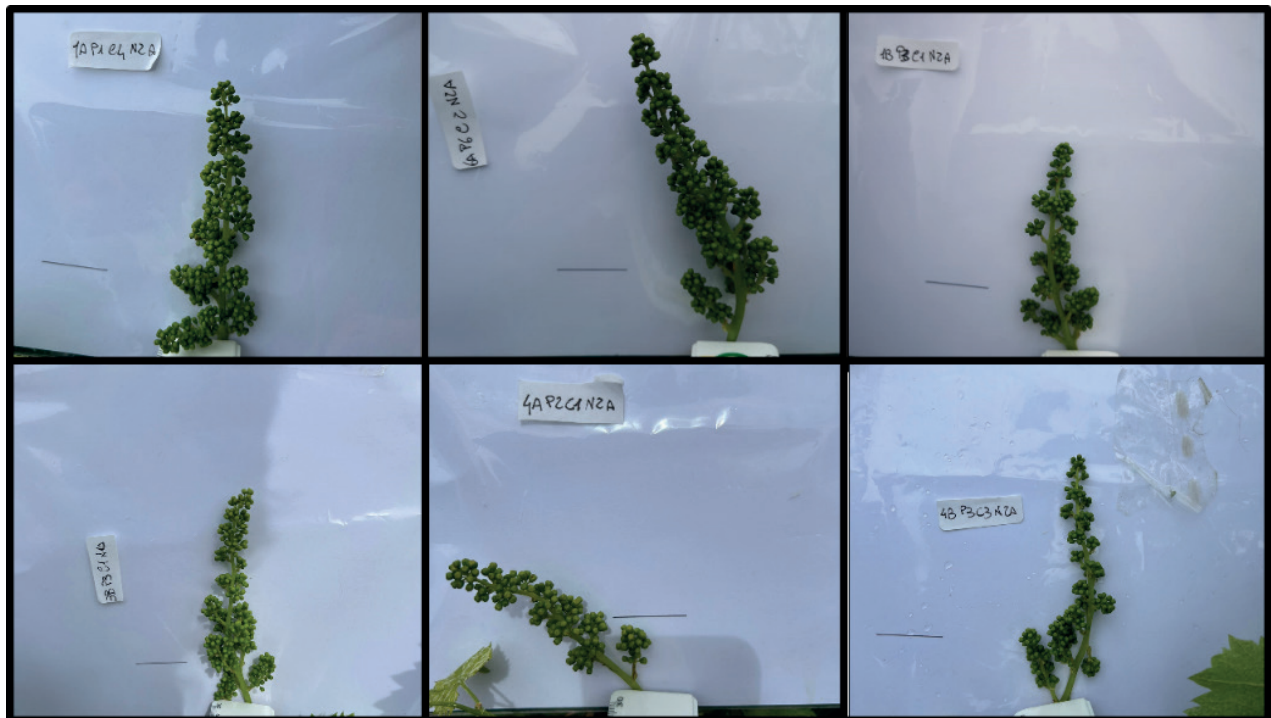


FIGURE 1. Images of Catarratto inflorescences acquired at BBCH 55 phenological stage according to the Lorenz scale (Lorenz *et al.*, 1995). Note the variability in terms of shape and size, as well as the lighting conditions of the scene. The black segment within the images indicates a length of 3 cm.

Afterwards, each inflorescence was covered with a tulle fabric net. The net was removed after complete flowering, and manual counting of detached calyptra was performed to validate the analysis. To externally validate the model (*i.e.*, to assess its prediction accuracy when applied to data from a dataset that was not used for training), images of an additional 70 Catarratto inflorescences from plants adjacent to the marked ones were randomly acquired under the same conditions. In addition, a dataset of images previously acquired in the same way, either in the vineyard (*in vivo*) or in the laboratory (*ex vivo*), was also used. This dataset included images of the cultivars Chardonnay (48 *in vivo* and 62 *ex vivo* images of inflorescences) and Vermentino (34 *ex vivo* images of inflorescences). For the external image dataset, only the number of flower buttons was counted.

2. Yield components

At harvest, the 36 marked Catarratto vines on which inflorescences (then bunches) were labelled were manually harvested. The total weight of the bunches was measured using a digital dynamometer (GC-60, LCD s.r.l., Italy). These were transported to the laboratory, where their weight was measured individually (Gibertini technical balance, EUC7500PT) and the relative number of berries counted. The fruit set rate was calculated on a plant basis in accordance with Palacios *et al.* (2020) as:

$$\% \text{ Fruit set rate} = \frac{\sum A_g}{\sum F_i} * 100 \quad (1)$$

where A_g represents the number of berries per bunch and F_i the number of flowers per inflorescence.

The flower density of each inflorescence was calculated as the ratio of the number of flowers to the length of the rachis, adapting a method originally proposed for bunch compactness by Pommer *et al.* (1996).

3. Image analysis

All images were pre-processed and analysed using the open-source FIJI/ImageJ® software (Schindelin *et al.*, 2012). Each image, with a resolution of 1536×2048 pixels, was first converted to grayscale (8-bit) to reduce the colour-related information (256 possible values) and facilitate segmentation (Image > Type > 8-Bit). The Region of Interest (ROI), which corresponds to the inflorescence, was then extracted through automatic thresholding using Otsu's method (Otsu, 1975; Nobuyuki, 1979), as described in the following equation:

$$ROI = \begin{cases} 0 & \text{if } I_b(x, y) \leq T_{otsu} \\ 255 & \text{otherwise} \end{cases} \quad (2)$$

where T_{otsu} represents the optimal threshold, determined by assuming the existence of only two classes of pixels within the image (one corresponding to the background and the other to the foreground). The goal is to find the threshold that maximises the variance between these two classes. I_b denotes the 8-bit image as a two-dimensional function in discrete space, with values ranging from 0 to 255. Using this approach, a binary image (0 = white and 255 = black) was generated, containing only the ROI and background pixels (Image > Adjust > Auto Threshold > Otsu). No parameters associated with the Otsu method were manually adjusted. The number of pixels in the ROI was then counted (Analyse > Measure). The flowchart related to image analysis can be summarised by the sequence shown in Figure 2.

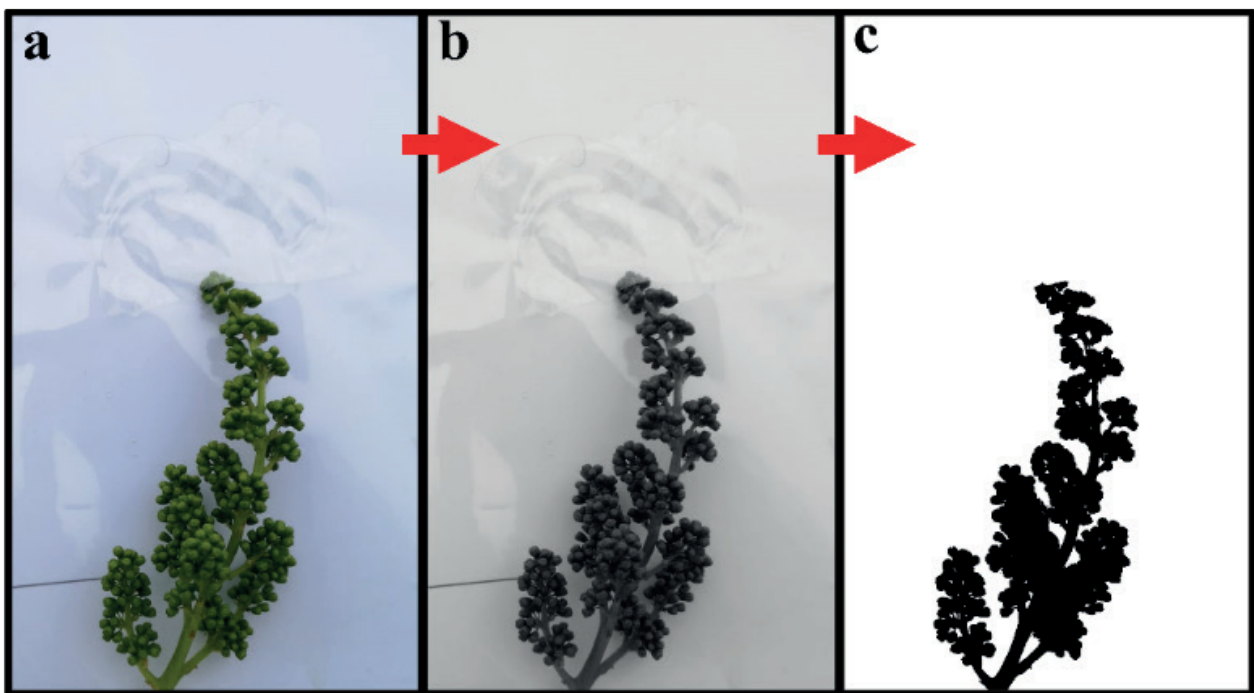


FIGURE 2. Flowchart of the main steps of the analysis. a, original image; b, image converted to grayscale (8-bit); c, segmented and binarised image using Otsu method (Otsu, 1975). Inflorescence of the Catarratto cultivar.

The only manual pre-processing step performed before thresholding was the removal of the dark reference line visible in the original image. This line was introduced for experimental purposes and does not appear in practical applications; therefore, its removal was necessary to avoid interference with the segmentation process and ensure accurate identification of the region of interest.

4. Statistical analysis

The data obtained were analysed using Minitab® version 19 statistical software (Minitab, USA). The distribution of inflorescence lengths was assessed using the Shapiro–Wilk normality test, with significance considered for $P \leq 0.05$. Correlations between the manually counted number of flowers, the number of pixels corresponding to inflorescences obtained through image segmentation, and inflorescence length were evaluated using linear regression models. Their coefficients of determination (R^2) were considered significant for $P \leq 0.01$. Root Mean Square Error (RMSE) and Mean Absolute Percentage Error (MAPE) were calculated to assess the error in the flower number prediction model, following the methodology of Paulus *et al.* (2014), using the equations provided below:

$$RMSE = \sqrt{\text{mean}(t - a)^2} \quad (3)$$

$$MAPE = \text{mean} \left(\left| \frac{t - a}{t} * 100 \right| \right) \quad (4)$$

where t (target) is the reference value; a (actual) is the predicted value.

The number of flowers predicted through the regression line equation, cumulated for the respective plant, was related to the number of berries and the cumulated bunch weight of the same plant using a linear regression model, and the corresponding coefficient of determination (R^2) considered significant for $P \leq 0.01$, similar to what was reported by Palacios *et al.*, (2020) for number of flowers/plant estimation in the perspective of yield component prediction. Leave-one-out cross-validation (LOOCV) was used to assess model accuracy. Flower number within rachis length classes was compared by analysis of variance (ANOVA) using the Tukey post-hoc test ($P < 0.05$).

TABLE 1. Classification of inflorescences based on length (L). The percentage (%) refers to the representativeness of the respective class within the total inflorescences sampled ($n = 300$).

Length class	Rachis length (cm)	%	Flowers (n)	Flower density
A	$L < 6$	14	131 ± 11.3 d	32.9 ± 2.8
B	$6 \leq L < 8$	14	272 ± 17.9 c	38.7 ± 2.7
C	$8 \leq L < 10$	18	287 ± 11.3 c	32.3 ± 1.3
D	$10 \leq L < 12$	25	399 ± 14.7 b	36.4 ± 1.3
E	$12 \leq L < 14$	15	446 ± 25.0 b	34.4 ± 1.9
F	$L \geq 14$	13	552 ± 29.2 a	35.2 ± 2.0

Different letters within columns indicate statistically significant differences at $P < 0.05$, according to Tukey's test. n.s. indicates no significant differences. The number of flowers and the inflorescence flower density are presented as mean \pm standard error.

RESULTS

1. Flower number prediction

Measurements taken prior to image acquisition showed that inflorescence lengths followed a normal distribution, as confirmed by the Shapiro–Wilk normality test, with a P -value above the threshold for statistical significance ($P > 0.1$). Based on this, six discrete length classes (L) were defined to cover the distribution, ensuring that for each class, the number of inflorescences represented at least 10 % of the total. Table 1 shows the length classes, the average number of flowers per inflorescence, and the average flower density within the relevant classes.

A positive linear correlation was observed between rachis length and flower count ($n = 300$) (Figure 3). However, within each length class, the number of flowers varies significantly, with variability that increases with inflorescence length. For instance, the flower count range extends from 274 in class A to 900 in class F. Notably, inflorescences with similar lengths (within a 2 cm range) exhibit progressively larger areas as the number of flowers increases. The regression between the number of ROI pixels and manually counted flowers confirms a strong linear relationship, yielding a R^2 of 0.78 even after performing LOOCV, a RMSE of 96.37 and a MAPE of 29.3 %, which decreased to 12.6 % when the correlation between actual and predicted flowers was performed on the total number of flowers per individual vine (Figure 3). As can be observed, higher flower numbers correspond to a significant increase in pixel area. However, for inflorescences containing fewer than 100 flowers, the data points generally lie below the regression line. This deviation likely results from the rachis contributing proportionally more to the total ROI area when flower numbers are low. Conversely, in more densely flowered inflorescences, the rachis has a reduced impact. This outcome reflects the inherent challenge of extracting data from a two-dimensional image of a three-dimensional structure. Additionally, inflorescence shape irregularity affects the proportion of hidden surface area, introducing variability based on image acquisition angle and asymmetry.

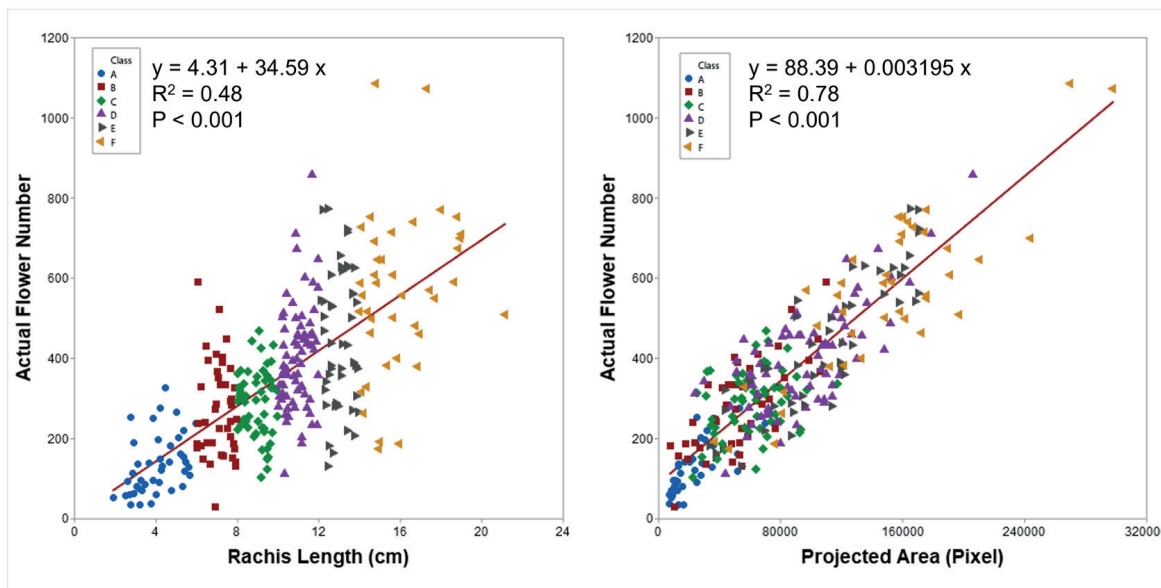


FIGURE 3. Correlation between manually counted flower number and rachis length (L) (left) and inflorescences ($n = 300$) projected area (right). A, $L < 6$ cm; B, $6 \leq L < 8$ cm; C, $8 \leq L < 10$ cm; D, $10 \leq L < 12$ cm; E, $12 \leq L < 14$ cm; F, $L \geq 14$ cm.

In Figure 4, the model equation shown in Figure 3 (where x corresponds to rachis length (L) and y to the actual number of flowers) was applied to predict the number of flowers in each class. A closer look at individual classes reveals that class C exhibits the lowest coefficient of determination (R^2), a non-significant P -value, and no clear correlation between the two variables. This is likely due to the lower variability in flower count within the 8–9.9 cm range, as indicated by a reduced standard error and lower flower density. Furthermore, prediction error decreases as inflorescence length and flower count increase. In class A, for example, the MAPE is 58.4 % (RMSE: 55 flowers; mean: 131 ± 73 flowers), whereas in class F, the MAPE drops to 18.7 % (RMSE: 105 flowers) despite a much higher mean of 562 ± 202 flowers per inflorescence. Overall, the results indicate that when flower count variability is low within a length class, prediction accuracy is primarily influenced by inflorescence morphology. Conversely, when variability is high, the model provides reliable approximations, as seen in classes E and F and in the overall trend across all length categories.

Model validation with external datasets further supports its predictive capability (Figure 5). For the Catarratto cultivar, the predicted flower count achieved an MAPE of 20 % and an RMSE of 68 flowers. However, performance declined with other cultivars. In Chardonnay, the *ex vivo* dataset exhibited a high MAPE relative to the mean, while the *in vivo* dataset showed better accuracy, aligning with the trends observed in Catarratto length classes. The lowest prediction accuracy was found in Vermentino, suggesting that cultivar-specific factors influence prediction performance.

2. Yield components prediction

The model based on the correlation between the total number of flowers per plant and the projected inflorescence area was also applied to predict plant-scale yield components (Figure 6).

The predictive model demonstrated high accuracy in estimating the number of berries per plant. The fruit set rate for each plant was used as a correction factor by multiplying the number of flowers obtained from the linear model by the corresponding fruit set percentage, following the approach of Millan *et al.* (2017) and Palacios *et al.* (2020), yielding a MAPE of 23.4 % and an R^2 0.93 after LOOCV. A less precise yet noteworthy result ($R^2 = 0.77$ after LOOCV, MAPE = 25.7 %) was obtained for bunch mass prediction. While the fruit set rate significantly influences berry count accuracy, in the case of bunch mass, the determining factor is average berry weight. Incorporating this additional correction factor would likely enhance accuracy, as suggested by Palacios *et al.* (2020).

DISCUSSION

To date, the most widely used methodology for estimating the number of flowers through image analysis mainly involves measuring the peaks of maximum brightness that floral buttons present compared to other elements in the images, due to their spheroidal shape (Millan *et al.*, 2017; Aquino *et al.*, 2015a; Aquino *et al.*, 2015b; Diago *et al.*, 2014). However, these brightness peaks are not always clearly visible or associated with a floral button, because a single button may have more than one peak, and the shape of these peaks is not always the same (spherical), causing the reflection magnitude to vary. This issue has already been pointed out by Liu *et al.* (2018), who found in their study that flower buttons of the Chardonnay cultivar in early phenological stages do not present any reflection peaks, while in the Syrah cultivar, more than two are present in more advanced phenological stages. This suggests that this may vary between cultivars and in relation to natural lighting conditions. Liu *et al.* (2018) overcame this problem by using

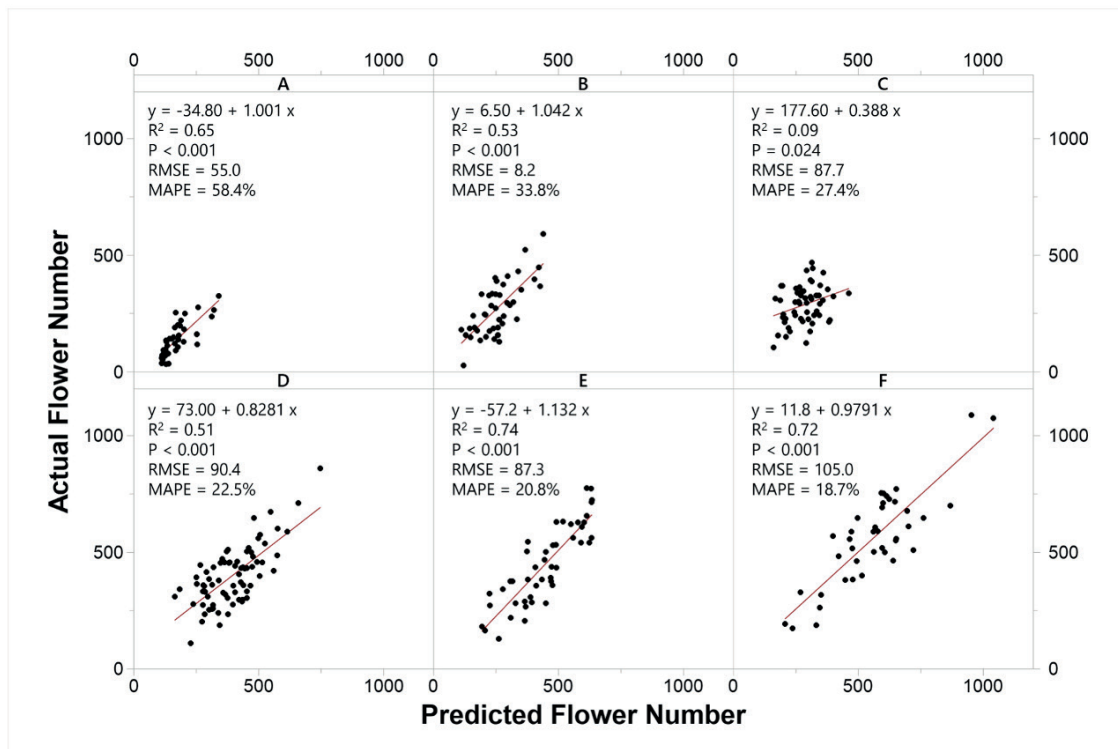


FIGURE 4. Correlation between the manually counted flower number and the predicted flower number within each length (L) class ($n = 300$). A, $L < 6$ cm; B, $6 \leq L < 8$ cm; C, $8 \leq L < 10$ cm; D, $10 \leq L < 12$ cm; E, $12 \leq L < 14$ cm; F, $L \geq 14$ cm.

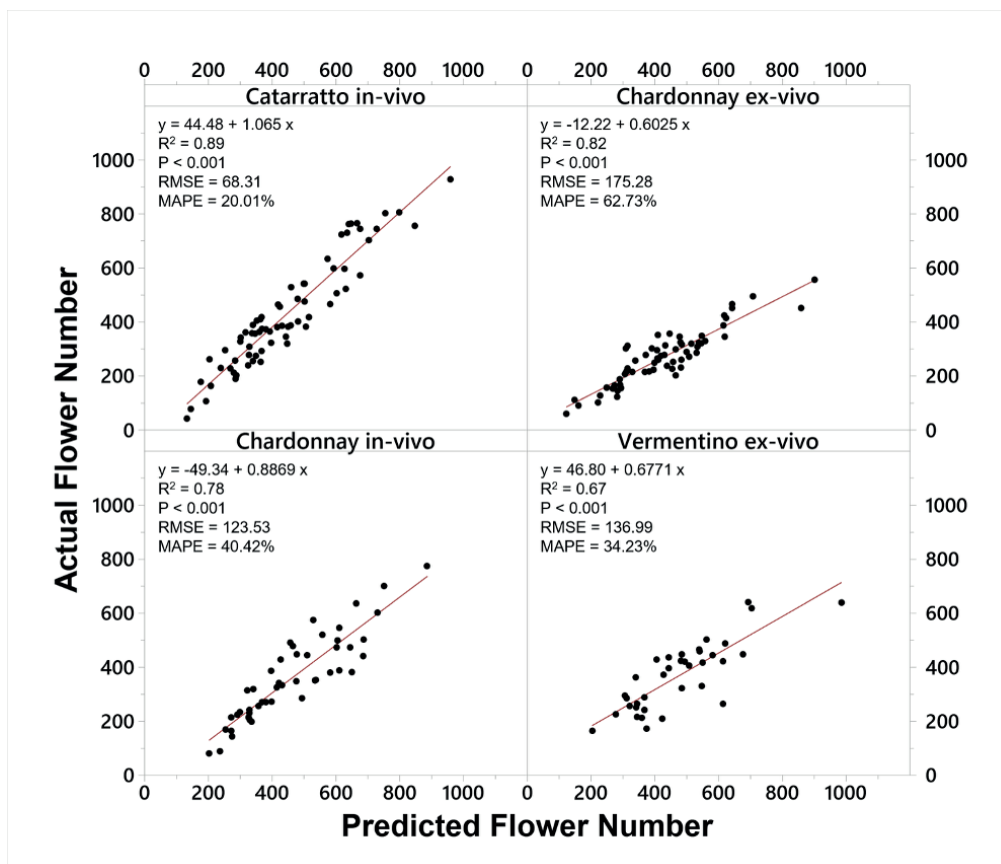


FIGURE 5. Correlation between the manually counted flower number and the predicted flower number in Catarratto inflorescences ($n = 70$) randomly sampled for external model validation, Chardonnay inflorescences predicted from in vivo images ($n = 48$) and ex vivo images ($n = 62$), and Vermentino inflorescences predicted from ex vivo images ($n = 34$).

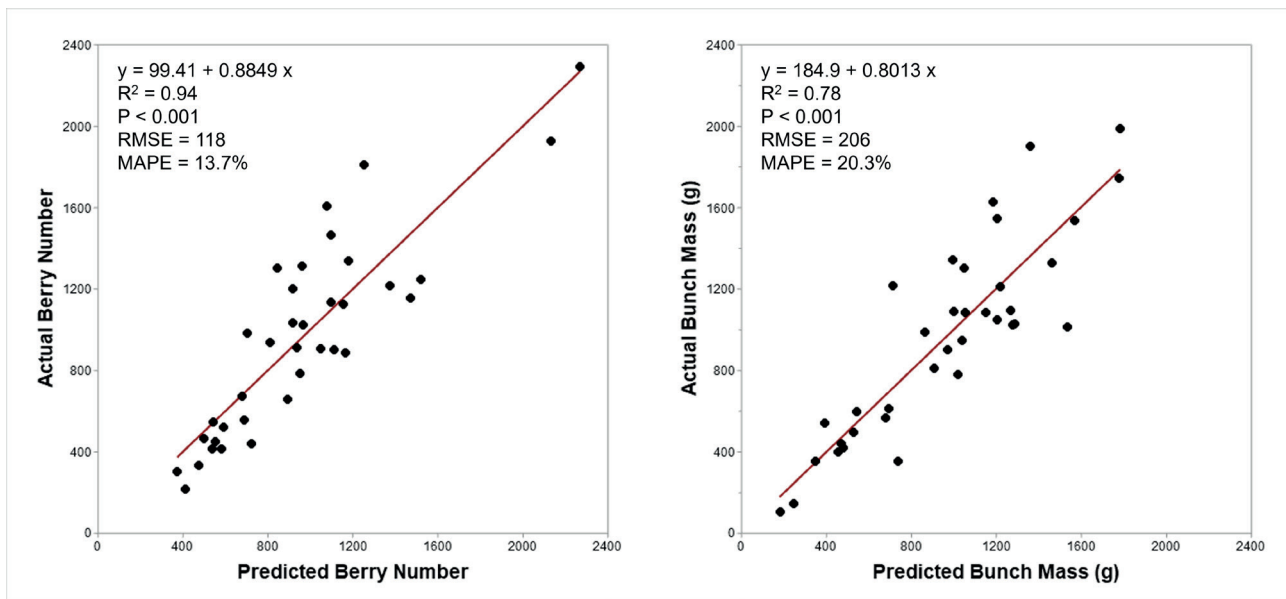


FIGURE 6. Correlation between the manually counted and predicted number of berries (left) and between actual and predicted bunch mass (right) per plant ($n = 36$). The values were corrected based on the fruit set rate of each plant.

different algorithms contextually, including the Speeded Up Robust Feature (SURF) algorithm, the Fast Retina Keypoint (FREAK) algorithm, and the Histogram of Oriented Gradients (HOG) algorithm, all of which are shape detectors used for object recognition in RGB images (Alahi *et al.*, 2012; Bay *et al.*, 2008; Dalal & Triggs, 2005). By doing so, they identified individual flower buttons morphologically, thus no longer relying on light reflection. In the present study, the adopted methodology was the simplest so far proposed: the images were segmented by simply isolating the entire inflorescence from the background, and the projected area (*i.e.*, the number of pixels) was used for correlation to estimate the total number of flowers. As the results showed, within the same class, in a range of about 2 cm inflorescence length, an increase in the number of flowers resulted in a more than proportional increase in the projected area. The nonsignificant differences in flower density found among the compared classes suggest that the above variability could not be attributed to different degrees of density or the size of individual flower buttons (Table 1). This approach effectively avoided the challenge of recognising individual flowers within the image and estimating false positives or false negatives. Moreover, the results obtained by other authors, who used the projected area of the inflorescence in combination with the visible flower button count for multi-factor modelling, suggest that a prediction methodology based solely on area, such as the one presented here, is applicable with satisfactory results (Tello *et al.*, 2020; Liu *et al.*, 2018). This avoids the bias associated with the manual setting of certain parameters in the analysis that characterises most estimation methods found in the literature, with clear positive repercussions on replicability and transferability. In the aforementioned studies, the number of flowers was estimated by relating this to the count of visible flowers in the image, without taking into account the relationship between the number of flowers

and the inflorescence size (Palacios *et al.*, 2020; Millan *et al.*, 2017; Aquino *et al.*, 2015a; Aquino *et al.*, 2015b; Diago *et al.*, 2014). Only a few authors also considered the density factor, but it was included directly as a factor in multiple regression models that still included the number of visible flowers among other factors (Tello *et al.*, 2020; Liu *et al.*, 2018). The model presented here is in line with models in the literature in terms of accuracy. A summary contrasting our method with representative studies is presented in Table 2. It should be emphasised that comparing models generated from different methodologies and datasets of varying sizes, in terms of number of cultivars, inflorescences, and population means, can lead to misinterpretations with respect to the goodness of the models themselves, especially if this is based solely on the comparison of R^2 values. Many of the proposed models, both linear monofactorial and especially nonlinear multifactorial, were generated from datasets whose studied populations ranged from fifteen to a hundred units. This is why some authors suggest using additional parameters, such as adjusted R^2 or MAPE, for comparison, understanding that any evaluation cannot disregard a clear knowledge of the distribution of the reference dataset (Liu *et al.*, 2018; Miles, 2005). Therefore, it is complicated to determine whether one method is superior to another. However, other factors can be considered, such as its transferability of the algorithm and its complexity. The images used in this study were processed without manually setting any parameters, allowing for transferability. A methodology that is analytically rapid and simple, like the one proposed, may have potential for application if implemented on an inexpensive mobile device, such as a smartphone, and validated on a larger number of cultivars and conditions. Additionally, results from other studies highlight that there is no advantage in using multiple factors in models and that linear models perform best (Liu *et al.*, 2018; Millan *et al.*, 2017).

TABLE 2. Comparative summary of recent studies applying image-based methods for inflorescence analysis and yield prediction in grapevine. The table reports the target variable, dataset size, cultivar diversity, modelling approach, model performance (R^2 , RMSE, and MAPE, when available), and whether yield component prediction was included.

Study	Target	Inflorescence (n)	Cultivar	Model	R^2	MAPE (%)	Yield components prediction
Present	ROI area	300 + 216	3	Linear	0.67 to 0.89	20.01 to 62.73	Yes
Diago <i>et al.</i> (2014)	Visible flower number	90	3	Linear	0.76	-	No
Aquino <i>et al.</i> (2015b)	Visible flower number	40	4	Linear – Nonlinear	0.85 to 0.95	-	No
Millan <i>et al.</i> (2017)	Visible flower number	132	11	Linear – Nonlinear	0.91	-	Yes
Liu <i>et al.</i> (2018)	Visible flower number + ROI area	204	4	Linear – Nonlinear	0.79 to 0.94	10.12 to 24.62	No
Tello <i>et al.</i> (2020)	Visible flower number + ROI area	460	19	Linear	0.83 to 0.91	14.4	No
Palacios <i>et al.</i> (2020)	Visible flower number	96	6	Linear	-	-	Yes

Regarding the development of cultivar-independent models, results obtained in other studies suggest that if inflorescence images are acquired at the same stage of development, this is possible if one considers 80 % estimation accuracy as a threshold for success (Tello *et al.*, 2020; Liu *et al.*, 2018). The validation of the model on external datasets carried out in the present study is consistent with these considerations, which is why future investigations should focus more on inflorescence morphology than on the development of more complex flower-detecting algorithms, as both flower size and inflorescence density are cultivar-specific traits that can significantly affect the accuracy of image-based quantification methods. Concerning the estimation of yield components, this study started by estimating the total number of flowers per plant, then estimating the corresponding number of berries and bunch weight. The results obtained, in agreement with those found by other authors on Cabernet-Sauvignon, Malvasia, Muscat of Alexandria, Syrah, Tempranillo, and Verdejo (Palacios *et al.*, 2020), support the idea that, through image analysis, it would be possible to develop more accurate models capable of predicting yield three to four months in advance. Clearly, such estimation also depends on factors unrelated to the parameters that can be deduced from an image. Indeed, the number of berries and bunch weight depend on the fruit set rate as well as on the season's weather pattern, the nutritional and water status of the plants, canopy management, and other external factors such as light and temperature (Krstic *et al.*, 2005; May, 2004; Coombe, 1972). However, modern viticulture can benefit from the use of vigour maps and associated prescription maps, which would allow calibration of yield estimation models to specific fruit set rates for the cultivar and soil and climate environment in which they operate. One of the limitations of applying this type of methodology, which has not been explored to date, is related to determining which and how many inflorescences and from which plants should be photographed to obtain a satisfactory estimate. The results obtained in the present study for yield estimation, as well as those in other studies (Palacios *et al.*, 2020), were obtained by capturing images of

100 % of a plant's inflorescences. However, it has been highlighted that inflorescences of different length classes can affect the accuracy of the estimation, and it has been observed that, in general, it is preferable to include inflorescences of widely varying lengths, though not going below 6 cm, as inflorescences shorter than this drastically reduce the accuracy of the estimation, affecting the result. For this reason, further studies should focus on determining the optimal threshold of inflorescences photographed per plant, with the understanding that applying the methodology to conditions where we already know the variability in the vineyard can help plan effective sampling schemes for each area.

CONCLUSION

In the present study, the results obtained highlight the following key findings: (i) the linear regression model developed shows significant promise in accurately estimating the number of flowers, particularly when considering the total flower count per plant. The methodology, if adapted for smartphone applications, could offer practical field-based solutions for yield prediction and production mapping. Camera angle and shooting distance can influence the estimation accuracy, as variations in these factors may alter the number of pixels representing the same inflorescence area, thereby reducing the precision of the analysis. However, this issue could be easily addressed in practical implementation. Tools such as ghost overlays (reference outlines shown on screen), digital inclinometers, or data from the phone's gyroscope and accelerometer could guide the user to capture images from consistent distances and angles. These features would help standardise image acquisition and improve the robustness of the method. For this methodology to be broadly applicable, however, it will need to be validated on a large scale across various cultivars, considering diverse flower shapes, sizes, and densities. Alternatively, cultivar-specific models may be developed for greater precision. The study also suggests that inflorescence length, a parameter

previously underexplored, could play a pivotal role in developing accurate models using straightforward analysis algorithms and simple linear correlations. (ii) the possibility of estimating yield components through regression models based on this approach appears promising; however, it is important to account for cultivar-specific and environmental factors that influence fruit set rate. Rather than offering a finalised methodology, the approach proposed in this work aimed to evaluate the potential of a simplified and adaptable pipeline for flower quantification based on image analysis. Identifying and testing alternative strategies at the flowering stage is considered a valuable step toward expanding the set of practical tools available for early yield prediction and facilitating their integration into more comprehensive and scalable systems.

ACKNOWLEDGEMENTS

The authors would like to express their gratitude to Tenuta Rapitalà, Camporeale (PA), Italy, for providing the vineyard and offering technical assistance.

REFERENCES

- Alahi, A., Ortiz, R., & Vanderghenst, P. (2012). Freak: Fast retina keypoint. In 2012 IEEE conference on computer vision and pattern recognition (pp. 510-517). IEEE. <https://doi.org/10.1109/CVPR.2012.6247715>
- Altherwy, Y. N., & McCann, J. A. (2020). SING: Free Space SensING of Grape Moisture using RF Shadowing. *IEEE Trans. Instrum. Meas.* 70, 6001112. <https://doi.org/10.1109/TIM.2020.3027928>
- Aquino, A., Millan, B., Diago, M.-P., & Tardaguila, J. (2018). Automated early yield prediction in vineyards from on-the-go image acquisition. *Computers and Electronics in Agriculture*, 144, 26–36. <https://doi.org/10.1016/j.compag.2017.11.026>
- Aquino, A., Millan, B., Gaston, D., Diago, M.-P., & Tardaguila, J. (2015a). vitisFlower®: Development and Testing of a Novel Android-Smartphone Application for Assessing the Number of Grapevine Flowers per Inflorescence Using Artificial Vision Techniques. *Sensors*, 15, 21204–21218. <https://doi.org/10.3390/s150921204>
- Aquino, A., Millan, B., Gutiérrez, S., & Tardaguila, J. (2015b). Grapevine flower estimation by applying artificial vision techniques on images with uncontrolled scene and multi-model analysis. *Computers and Electronics in Agriculture*, 119, 92–104. <https://doi.org/10.1016/j.compag.2015.10.009>
- Bay, H., Ess, A., Tuytelaars, T., & Van Gool, L. (2008). Speeded-up robust features (SURF). *Computer Vision and Image Understanding*, 110(3), 346–359. <https://doi.org/10.1016/j.cviu.2007.09.014>
- Benmehaia, R., Khedidja, D., & Bentchikou, M. E. M. (2016). Estimation of the flower buttons per inflorescences of grapevine (*Vitis vinifera* L.) by image auto-assessment processing. *African Journal of Agricultural Research*, 11, 3203–3209. <https://doi.org/10.5897/AJAR2016.11331>
- Bennett, J., Jarvis, P., Creasy, G. L., & Trought, M. C. (2005). Influence of defoliation on overwintering carbohydrate reserves, return bloom, and yield of mature Chardonnay grapevines. *American Journal of Enology and Viticulture*, 56, 386–393. <https://doi.org/10.5344/ajev.2005.56.4.386>
- Bessis, R. (1960). Two rapid methods of estimating the number of flowers in vine inflorescences. *C. r. Hebd. Seances Acad. Agric. Fr.*, 46, 823–8.
- Carrillo, E., Matese, A., Rousseau, J., & Tisseyre, B. (2016). Use of multi-spectral airborne imagery to improve yield sampling in viticulture. *Precision Agriculture*, 17, 74–92. <https://doi.org/10.1007/s11119-015-9407-8>
- Clingeffer, P. R. (2010). Plant management research: status and what it can offer to address challenges and limitations. *Australian Journal of Grape and Wine Research*, 16, 25–32. <https://doi.org/10.1111/j.1755-0238.2009.00075.x>
- Clingeffer, P. R., & Krstic, M. (2003). Crop development, crop estimation and crop control to secure quality and production of major wine grape varieties: a national approach: final report to Grape and Wine Research & Development Corporation. Grape and Wine Research and Development Corporation: Adelaide, Australia.
- Coombe, B. (1972). The regulation of set and development of the grape berry. *Acta Horticulturae*, 34: Symposium on growth Regulators in Fruit Production, 261–274. <https://doi.org/10.17660/ActaHortic.1973.34.36>
- Cubero, S., Diago, M., Blasco, J., Tardaguila, J., Prats-Montalbán, J., & Ibáñez, J. (2015). A new method for assessment of bunch compactness using automated image analysis. *Australian Journal of Grape and Wine Research*, 21, 101–109. <https://doi.org/10.1111/ajgw.12118>
- Dalal, N., & Triggs, B. (2005). Histograms of oriented gradients for human detection. *Computer Society Conference on Computer Vision and Pattern Recognition (CVPR'05)*, 886–893. <https://doi.org/10.1109/CVPR.2005.177>
- De La Fuente, M., Linares, R., Baeza, P., Miranda, C., & Lissarrague, J. R. (2015). Comparison of different methods of grapevine yield prediction in the time window between fruitset and veraison. *OENO One*, 49, 27. <https://doi.org/10.20870/oeno-one.2015.49.1.96>
- Demestihias, C., Debuissou, S., Descotes, A. (2018). Decomposing the notion of vine vigour with a proxydetection shoot sensor: Physiocap®. In *Proceedings of the E3S Web of Conferences*, Polanica-Zdrój, Poland, 16–18 April. <https://doi.org/10.1051/e3sconf/20185003003>
- Diago, M.-P., Tardaguila, J., Aleixos, N., Millan, B., Prats Montalbán, J., Cubero, S., Blasco, J. (2015). Assessment Of Cluster Yield Components By Image Analysis. *J. Sci. Food Agric.*, 95. <https://doi.org/10.1002/jsfa.6819>
- Diago, M., Sanz-Garcia, A., Millan, B., Blasco, J., & Tardaguila, J. (2014). Assessment of flower number per inflorescence in grapevine by image analysis under field conditions. *Journal of the Science of Food and Agriculture*, 94, 1981–1987. <https://doi.org/10.1002/jsfa.6512>
- Dunn, G. M., & Martin, S. R. (2004). Yield prediction from digital image analysis: A technique with potential for vineyard assessments prior to harvest. *Australian Journal of Grape and Wine Research*, 10, 196–198. <https://doi.org/10.1111/j.1755-0238.2004.tb00022.x>
- Dunn, G. M., & Martin, S. R. (2007). A functional association in *Vitis vinifera* L. cv. Cabernet Sauvignon between the extent of primary branching and the number of flowers formed per inflorescence. *Australian Journal of Grape and Wine Research*, 13, 95–100. <https://doi.org/10.1111/j.1755-0238.2007.tb00239.x>
- Fernandez, R., Montes, H., Salinas, C., Sarria, J., Armada, M. (2013). Combination of RGB and Multispectral Imagery for Discrimination of Cabernet Sauvignon Grapevine Elements. *Sensors*, 13, 7838–7859. <https://doi.org/10.3390/s130607838>
- Font, D., Pallejà, T., Tresanchez, M., Teixidó, M., Martínez, D., Moreno, J., Palacín, J. (2014). Counting red grapes in vineyards by detecting specular spherical reflection peaks in RGB images obtained at night with artificial illumination. *Comput. Electron. Agric.*, 108, 105–111. <https://doi.org/10.1016/j.compag.2014.07.006>

- Henry, D., Aubert, H., Véronèse, T. (2019). Proximal Radar Sensors for Precision Viticulture. *IEEE Trans. Geosci. Remote Sens.*, 57, 4624–4635. <https://doi.org/10.1109/TGRS.2019.2891886>
- Howell, G. S. (2001). Sustainable Grape Productivity and the Growth-Yield Relationship: A Review. *American Journal of Enology and Viticulture*, 52, 165–174. <https://doi.org/10.5344/ajev.2001.52.3.165>
- Keller, M. (2010). Managing grapevines to optimise fruit development in a challenging environment: a climate change primer for viticulturists. *Australian Journal of Grape and Wine Research*, 16, 56-69. <https://doi.org/10.1111/j.1755-0238.2009.00077.x>
- Kliwer, W. M., & Dokoozlian, N. K. (2005). Leaf Area/Crop Weight Ratios of Grapevines: Influence on Fruit Composition and Wine Quality. *American Journal of Enology and Viticulture*, 56, 170–181. <https://doi.org/10.5344/ajev.2005.56.2.170>
- Kliwer, W., & Casteel, T. (2003). Canopy management. *Oregon Viticulture. EW Hellman (Ed.)*, 177-184.
- Krstic, M., Clingeleffer, P., Dunn, G., Martin, S., & Petrie, P. (2005). Grapevine growth and reproductive development: an overview. In ‘Transforming flowers to fruit’. ASVO Proceedings, 7-10.
- Liu, S. (2017). Automated yield estimation in viticulture by computer vision. PhD Thesis. UNSW Sydney. <https://doi.org/10.26190/unswworks/3097>
- Liu, S., & Whitty, M. (2015). Automatic grape bunch detection in vineyards with an SVM classifier. *Journal of Applied Logic*, 13, 643–653. <https://doi.org/10.1016/j.jal.2015.06.001>
- Liu, S., Li, X., Wu, H., Xin, B., Tang, J., & Petrie, P. R. (2018). A robust automated flower estimation system for grape vines. *Biosystems Engineering*, 172, 110–123. <https://doi.org/10.1016/j.biosystemseng.2018.05.009>
- Lopes, C. M., & Cadima, J. (2021). Grapevine bunch weight estimation using image-based features: comparing the predictive performance of number of visible berries and bunch area. *Oeno One*, 55(4), 209-226. <https://doi.org/10.20870/oeno-one.2021.55.4.4741>
- Lopes, C., Graça, J., & Monteiro, A. (2021). Accurate estimation of grapevine bunch weight using image analysis: a case study with two Portuguese cultivars. *Acta Horticulturae*, 1314, 117-124. <https://doi.org/10.17660/ActaHortic.2021.1314.16>
- Lorenz, D., Eichhorn, K., Bleiholder, H., Klose, R., Meier, U., & Weber, E. (1995). Phänologische Entwicklungsstadien der Weinrebe (*Vitis vinifera* L. ssp. *vinifera*). Codierung und Beschreibung nach der erweiterten BBCH-Skala. *Wein-Wissenschaft*, 49, 66–70.
- May, P. (2000). From bud to berry, with special reference to inflorescence and bunch morphology in *Vitis vinifera* L. *Australian Journal of Grape and Wine Research*, 6, 82–98. <https://doi.org/10.1111/j.1755-0238.2000.tb00166.x>
- May, P. (2004). Flowering and fruitset in grapevines. Lythrum Press, Adelaide (Australia).
- Miles, J. (2005). “R-Squared, Adjusted R-Squared,” in *Encyclopedia of Statistics in Behavioral Science*, John Wiley & Sons, Ltd. <https://doi.org/10.1002/0470013192.bsa526>
- Millan, B., Aquino, A., Diago, M. P., & Tardaguila, J. (2017). Image analysis-based modelling for flower number estimation in grapevine. *Journal of the Science of Food and Agriculture*, 97, 784–792. <https://doi.org/10.1002/jsfa.7797>
- Millan, B., Velasco-Forero, S., Aquino, A., & Tardaguila, J. (2018). On-the-Go Grapevine Yield Estimation Using Image Analysis and Boolean Model. *Journal of Sensors*, 2018, 9634752. <https://doi.org/10.1155/2018/9634752>
- Moreno, H., Rueda-Ayala, V., Ribeiro, A., Bengochea-Guevara, J., Lopez, J., Peteinatos, G., Valero, C., Andújar, D. (2020). Evaluation of Vineyard Cropping Systems Using On-Board RGB-Depth Perception. *Sensors*, 20, 6912. <https://doi.org/10.3390/s20236912>
- Nobuyuki, O. (1979). A Threshold Selection Method From Gray-Level Histograms. *Transactions on Systems, Man, and Cybernetics*, 9, 62. <https://doi.org/10.1109/TSMC.1979.4310076>
- Nuske, S., Wilshusen, K., Achar, S., Yoder, L., Narasimhan, S., & Singh, S. (2014). Automated visual yield estimation in vineyards. *Journal of Field Robotics*, 31, 996. <https://doi.org/10.1002/rob.21541>
- Otsu, N. (1975). A threshold selection method from gray-level histograms. *Automatica*, 11, 23–27.
- Palacios, F., Bueno, G., Salido, J., Diago, M., Hernández, I., & Tardaguila, J. (2020). Automated grapevine flower detection and quantification method based on computer vision and deep learning from on-the-go imaging using a mobile sensing platform under field conditions. *Computers and Electronics in Agriculture*, 178, 105796. <https://doi.org/10.1016/j.compag.2020.105796>
- Parr, B., Legg, M., Alam, F., Bradley, S. (2020). Acoustic Identification of Grape Clusters Occluded by Foliage. In *Proceedings of the 2020 IEEE Sensors Applications Symposium (SAS)*, Kuala Lumpur, Malaysia, 9–11 March; pp. 1–6. <https://doi.org/10.1109/SAS48726.2020.9220078>
- Paulus, S., Behmann, J., Mahlein, A. K., Plümer, L., & Kuhlmann, H. (2014). Low-cost 3D systems: suitable tools for plant phenotyping. *Sensors*, 14(2), 3001-3018. <https://doi.org/10.3390/s140203001>
- Poblete-Echeverría, C., Berry, A., Venter, T., Velez, S., Pavez, M. I. G., & Iñiguez, R. (2025). Morphological image analysis for estimating grape bunch weight under different irrigation regimes in Cabernet-Sauvignon: This article is part of the special issue of the GIESCO 2025 meeting. *OENO One*, 59(2). <https://doi.org/10.20870/oeno-one.2025.59.2.9309>
- Pommer, C. V., Pires, E. J. P., Terra, M. M., & Passos, I. R. S. (1996). Streptomycin-induced seedlessness in the grape cultivar Rubi (Italia Red). *American Journal of Enology and Viticulture*, 47, 340–342. <https://doi.org/10.5344/ajev.1996.47.3.340>
- Poni, S., Casalini, L., Bernizzoni, F., Civardi, S., & Intrieri, C. (2006). Effects of early defoliation on shoot photosynthesis, yield components, and grape composition. *American Journal of Enology and Viticulture*, 57, 397–407. <https://doi.org/10.5344/ajev.2006.57.4.397>
- Schindelin, J., Arganda-Carreras, I., Frise, E., Kaynig, V., Longair, M., Pietzsch, T. (2012). Fiji: an open-source platform for biological-image analysis. *Nature Methods*, 9, 676–682. <https://doi.org/10.1038/nmeth.2019>
- Tello, J., Herzog, K., Rist, F., This, P., & Doligez, A. (2020). Automatic Flower Number Evaluation in Grapevine Inflorescences Using RGB Images. *American Journal of Enology and Viticulture*, 71, 10–16. <https://doi.org/10.5344/ajev.2019.19036>
- Tello, J., Montemayor, M. I., Forneck, A., & Ibáñez, J. (2018). A new image-based tool for the high throughput phenotyping of pollen viability: evaluation of inter- and intra-cultivar diversity in grapevine. *Plant Methods*, 14, 3. <https://doi.org/10.1186/s13007-017-0267-2>
- Victorino, G., Braga, R., Santos-Victor, J., & Lopes, C. M. (2020). Yield components detection and image-based indicators for non-invasive grapevine yield prediction at different phenological phases. *OENO One*, 54(4), 833-848. <https://doi.org/10.20870/oeno-one.2020.54.4.3616>
- Victorino, G., Poblete-Echeverría, C., & Lopes, C. M. (2022). A multicultivar approach for grape bunch weight estimation using image analysis. *Horticulturae*, 8(3), 233. <https://doi.org/10.3390/horticulturae8030233>